Excited state refraction of C_{70}/toluene studied by using $4f$ coherent imaging system with phase object*

Liu Nan-Chun(刘南春)[a], Shi Guang(石 光)[b],
Yang Jun-Yi(杨俊义)[a], and Song Ying-Lin(宋瑛林)[a)b)†]

[a] *School of Physical Science and Technology, Suzhou University, Suzhou* 215006, *China*
[b] *Department of Physics, Harbin Institute of Technology, Harbin* 150001, *China*

(Received 31 January 2010; revised manuscript received 26 March 2010)

Dynamic nonlinearities of C_{70}/toluene solution are measured and analysed by an improved picosecond time-resolved pump-probe system based on a nonlinear imaging technique with phase object. The photophysical parameters are determined by the five-level model, which is adopted to interpret the experimental data. The change of refraction index per unit density of the excited state obtained by a numerically simulation is a critical factor to determine the nonlinear behaviour of C_{70} in picosecond time regime.

Keywords: $4f$ system, excited state refraction, C_{70}/toluene solution, refraction index per unit density

PACS: 31.70.Hg, 42.70.Mp, 42.65.–k **DOI:** 10.1088/1674-1056/20/1/013103

1. Introduction

Since the 1990's, the nonlinear absorption of fullerenes[1−9] has been studied and understood clearly. At the same time, the nonlinear refraction of fullerenes has not been comprehended completely. The reported values of third-order nonlinear susceptibility $\chi^{(3)}$ and nonlinear refractive index of fullerenes are shown to have a wide range each. The various results in different measurements are probably due to the following reasons. The nonlinear parameters are sensitive to the magnitude of the light intensity. Since the excited molecules play an increasing important role as the pulse width increases, a wide range of pulse width (from femtosecond to nanosecond) used in various experiments should yield different results. Various measurement techniques (DFWM, third harmonic generation, Z-scan) and spectral dispersion may also present different results. The nonlinearity of host material, such as, toluene, polymer and organometallic film, has also influence on the overall nonlinear characteristics of the fullerene-containing samples. In previous studies, the confusion was explained by the influence of additional nonlinear processes (thermal effects, Stark effect, etc.) other than the pure electronic Kerr effect. Based on the consideration that the density of excited singlet and triplet molecules determines the nonlinear refraction of C_{70}/toluene, a new parameter, which is defined as the change of refraction index per unit density, is introduced into the theoretical model to interpret the excited state refraction in this work. This parameter can determine the sign of nonlinear refraction naturally. A newly developed technique is adopted in the nonlinearity measurement.

A nonlinear-imaging single-shot technique (NIT) based on a $4f$ coherent imaging system to measure nonlinear optical properties has been developed by Boudebs *et al.*[10] A modified system, into which the $4f$ nonlinear imaging technique with phase object (NIT-PO) is incorporated, with a time delayed pump-probe technique, has been presented in Refs. [11]–[15] recently. The improved technique of greater signal sensibility can be used to measure the nonlinear absorption and refraction at the same time. Another vital advantage of the technique is that it can extract information about both the magnitude and the sign of the nonlinear coefficients simultaneously.

In this paper, we investigate the dynamic nonlinearities of C_{70}/toluene solution by the time-resolved pump-probe system based on $4f$ NIT-PO. The excited-state dynamics of the nonlinear samples is studied completely. A five-level model is adopted to describe the optical spectral response of the C_{70} molecule. The index of refraction is determined to help us to understand the nonlinear behaviour of C_{70} molecules.

*Project supported by the National Natural Science Fundation of China (Grant No. 90922007).
†Corresponding author. E-mail: ylsong@hit.edu.cn
© 2011 Chinese Physical Society and IOP Publishing Ltd

2. Experiment

The arrangement of the time-resolved pump-probe system to which a $4f$ NIT-PO system is incorporated, is shown in Fig. 1, and it is the same as that in previous work.[11−15] The optical source of the experiment is a frequency-doubled beam ($\lambda = 532$ nm) with a pulse width of 21 ps, irradiating from a Q-switched and mode-locked Nd:YAG laser (EKSPLA PL2143A). It is split into an intense pump beam and a much weaker probe one. The polarization of the pump beam is adjusted in the direction perpendicular to the probe beam by a half-wave plate. The spatial distribution of the laser beam is an approximately Gaussian beam distribution. The probe beam passes through a typical $4f$ system with a PO, which consists of convex lenses L_1 and L_2 with equal focal length $f_1 = f_2 = 40$ cm. The aperture with a radius $R_a = 1.7$ mm, in the middle a PO with a radius $L_p = 0.5$ mm gives a fixed phase retardation $\varphi = 0.4\ \pi$, is placed in the front focal plane of L_1. Only a small portion of the expanded weak probe laser can pass through the aperture in the centre. Since the radius of the expanded probe beam is much greater than the aperture, the laser beam illuminating the aperture can be considered as a top-hat one. And the nonlinear sample is placed in the Fourier plane of the $4f$ system.

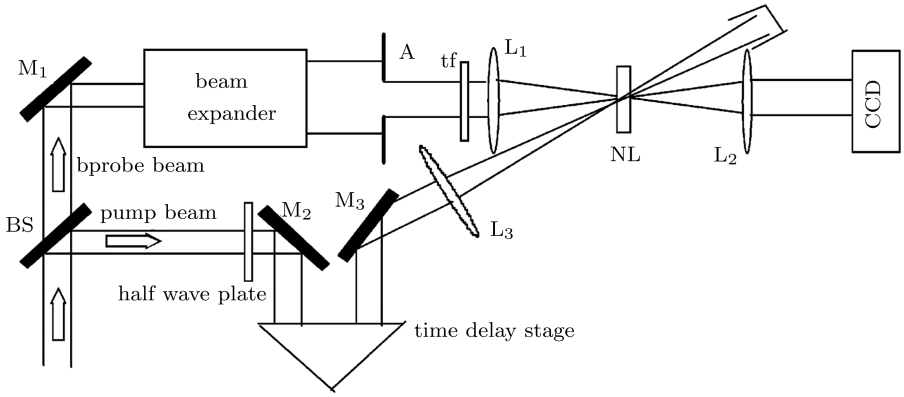


Fig. 1. Schematic of the time-resolved pump-probe system based on $4f$ nonlinear imaging technique with phase object. BS denotes the beam splitter, M_1–M_3 mirrors, L_1–L_3 convex lenses, A the aperture with phase object, tf the neutral filter, and NL the nonlinear sample.

A charge-coupled device (CCD, Imager QE of Lavision Company in Germany), which has 1040 × 1376 pixels and a 4095 gray level, is placed in the rear focal plane of L_2 to collect the image of probe beam. The nonlinear phase shift generated by the nonlinear sample is modulated into the amplitude change of the optical field and received by the CCD. The difference in the mean value of the normalized intensity between inside the PO and outside the PO is denoted as ΔT. The amplitude of ΔT increases with the induced nonlinear phase shift $\Delta\Phi$ within the sample. If $\Delta\Phi$ is positive, one has $\Delta T > 0$. Inversely, $\Delta T < 0$ while $\Delta\Phi$ is negative. Then, a numerically fitting method is adopted to calculate ΔT so as to deduce the nonlinear phase shift $\Delta\Phi$.

As mentioned in Ref. [12], the ratio ω_e/ω_p (ω_e is the radius of the pump beam and ω_p is the radius of the probe beam) plays an important role in determining the sensitivity of the measurement. The best choice of this ratio is about 2–3. Thus, both the nonlinear absorption and the refraction can reach relatively high sensitivities. In this experiment, the Airy radius of the probe beam in the Fourier plane is $\omega_p = 0.61\lambda f_1/R_a = 76\ \mu$m and the spot size of the focused probe beam with a spatial Gaussian profile is $\omega_e = 180\ \mu$m (HW $1/e^2$). Thus, the 2 mm-thick sample can be considered as a 'thin' one. A pinhole is necessary to ensure the accurate spatial overlap of the pump and the probe beams inside the nonlinear sample. The angle between the pump beam and the probe beams is 4.5°, and the intensity of the probe beam is approximately 1.5% of that of the pump beam. In order to ensure the accuracy, the experiments are carried out in a darkroom and the background light is also zeroed by software.

In the experiment, three images are recorded to

deduce the photophysical parameters by numerical simulation. Firstly, a linear image is obtained while a neutral filter is placed before the sample to attenuate the optical intensity. Thus, the laser intensity is too weak to induce the nonlinearity. Secondly, a nonlinear image is obtained by placing the same neutral filter behind the nonlinear material. Thirdly, a no-sample image is obtained by taking away the sample while the neutral filter remains there.

The number density of C_{70} molecules in this work is 7.32×10^{22}. In the experiment, the energy of a single pump pulse is 10.33 μJ, and it produces a peak intensity of 0.70 GW/cm^2.

3. Theory and discussion

In order to interpret the experimental results, a theoretical model and the relevant expressions are briefly reviewed. Polar coordinate is used in this work to facilitate calculations because of the circular symmetry of the pump beam and the probe beam. And, Fourier optics is used to describe the image formation in $4f$-NIT-PO. Because the nonlinear refractive index relaxes with a finite relaxation time, the dynamic phase grating, which is induced by the real part of the refractive index, yields a phase shift as the beams propagate through the medium.

In this work, the pump beam has a polarization linearly perpendicular to that of the probe beam. After exiting the PO, the optical field of the probe beam, which has a top-hat spatial profile, can be expressed as

$$\begin{aligned} A_{p0}(r,t) \;=\; & A_0 \;\exp(-t^2/2\tau_{\rm p}^2)\;\mathrm{circ}(r/R_{\rm a}) \\ & \times\; \exp[\mathrm{i}\varphi\;\mathrm{circ}(r/L_{\rm p})], \end{aligned} \tag{1}$$

where the subscript 0 means no pump beam; $A_0 = (E_0/\pi^{3/2}R_{\rm a}^2\tau_{\rm p})^{1/2}$ with E_0 being the pulse energy; $\tau_{\rm p}$ the laser pulse width (HW $1/e$ M); $\mathrm{circ}(x)$ is the circular function that has a value of one if $x \le 1$ and zero, otherwise; φ is the phase shift introduced by the PO, which is equal to $0.4\,\pi$ here; $R_{\rm a}$ and $L_{\rm p}$ are the radii of the aperture and the PO, respectively. The field in the focal plane of L_1 is the spatial Fourier transform of $A_{\rm p0}(r,t)$ expressed as

$$A_{\rm p0}(\rho,t) = \frac{2\pi}{\lambda f_1}\int_0^{R_{\rm a}} rA_{\rm p0}(r,t)\mathrm{J}_0(2\pi r\rho)\mathrm{d}r, \tag{2}$$

where λ is the wavelength of the probe beam, J_0 is the zero-order Bessel Function, and $\rho = r/\lambda f_1$ is the spatial frequency at the Fourier plane. The optical field of the probe beam given in Eq. (2) induces a circular grating on the sample with the thickness equal to L, which is placed in the focal plane of L_1. Thus, neglecting the linear and the nonlinear absorptions, the optical field exiting from the sample in the absence of the pump beam is expressed as

$$A_{\rm pL}(\rho,t) = A_{\rm p0}(\rho,t)\;\exp(\mathrm{i}\;\Delta\varphi_{\rm NL}) \tag{3}$$

where $\Delta\varphi_{\rm NL}$ is the nonlinear phase shift. At the output of the $4f$-NIT-PO (on the surface of CCD), the complex optical field is the inverse Fourier transform of $A_{\rm pL}(\rho,t)$, i.e.,

$$A_{\rm pL}(r,t) = 2\pi\lambda f_2\int_0^\infty \rho A_{\rm pL}(\rho,t)\mathrm{J}_0(2\pi r\rho)\mathrm{d}\rho. \tag{4}$$

So, the normalized fluence is given by

$$\begin{aligned} \mathrm{NF}(r) \;&=\; \frac{\int_{-\infty}^{+\infty}|A_{\rm pL}(r,t)|^2\mathrm{d}t}{T_0\int_{-\infty}^{+\infty}|A_{\rm p0}(r,t)|^2\mathrm{d}t} \\ &=\; \frac{\int_{-\infty}^{+\infty} I_{\rm pL}(r,t)\;\mathrm{d}t}{I_0\sqrt{\pi}\tau T_0} \end{aligned} \tag{5}$$

where $I_{\rm pL}(r,t)$ is the intensity of the probe beam impinging received by the CCD. The functions of time delay $t_{\rm d}$, $I_{\rm pL}(r,t)$ and $\mathrm{NF}(r)$ are not written out explicitly for brevity. In this work, ΔT, which is defined as the difference in the mean value of the fluence (transmitted energy per unit area) between inside the PO and outside the PO, is obtained through the numerical simulation of the nonlinear image by Eq. (5).

We also obtain the normalized transmitted energy (NT) expressed as

$$\mathrm{NT} = \frac{E_{\rm nl}}{E_{\rm l}} = \frac{2\pi\int_{-\infty}^{+\infty}\mathrm{d}t\int_0^\infty rI_{\rm pL}\mathrm{d}r}{E_0T_0}, \tag{6}$$

where $E_{\rm nl}$ can be obtained by integrating all the pixels of the nonlinear image, and $E_{\rm l}$ is obtained in the same manner in the absence of the pump beam.

A five-level system model as shown in Fig. 2 is adopted to interpret the nonlinear absorption refraction of C_{70} molecule. The pump beam pulse excites the C_{70} molecules from ground state S_0.

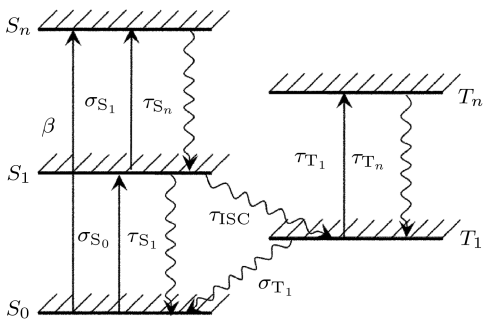


Fig. 2. Energy-level diagram of a C_{70} molecule.

From state S_1, the molecules will rapidly relax back to S_0 or undergo intersystem-crossing transition to the lowest excited triplet state T_1 through a spin-flip process. Otherwise, they are promoted to higher excited state S_n (where $n \geq 2$) by absorbing photons (excited-state absorption). The molecules in state T_1 can also be excited to a higher triplet state T_n. For the short lifetimes of S_n and T_n (<ps), the above exciting processes and relaxations of states S_n and T_n are negligible. However, the relaxation of T_1 to S_0 is forbidden and therefore very slow. The triplet state T_1, which has a long lifetime and larger absorption cross-section than the ground state, will accumulate significant population and eventually become a dominant absorption source. If the two-photon absorption (TPA, with coefficient expressed by β (m/W)) and Kerr refraction (n_2 (m^2/W)) are considered, equations to calculate intensity $I_p(\rho, t)$ and phase $\phi_p(\rho, t)$ can be obtained as

$$\frac{dI_p}{dz} = -\left(\sigma_{S_0} N_{S_0} + \sigma_{S_1} N_{S_1} + \sigma_{T_1} N_{T_1} + 2\beta I_e\right) I_p, \quad (7)$$

$$\frac{d\phi_p}{dz} = k(\Delta\eta_{S_1} N_{S_1} + \Delta\eta_{T_1} N_{T_1} + 2n_2 I_e), \quad (8)$$

where the factors of 2 before β and n_2 come from weak-wave retardations and their validities depend on the condition that the response time of the medium τ_r must be shorter than the beat period, i.e., $\tau_r \, |\omega_p - \omega_e| << 1$.[16,17] In the present work, it is true for degenerate or instantaneous nonlinearities. The intensity depletion equation of the pump beam is expressed as

$$\frac{dI_e}{dz} = -\left(\sigma_{S_0} N_{S_0} + \sigma_{S_1} N_{S_1} + \sigma_{T_1} N_{T_1} + \beta I_e\right) I_e, \quad (9)$$

where N_i denotes the population density of state i, which has a corresponding absorption cross section σ_i; $\Delta\eta_i$ denotes the change of refraction index per unit density of state I; z is the propagation length of laser within the sample.

The rate equations should be numerically solved first. Then, together with Eqs. (7)–(9), $I_{pL}(\rho, t)$ and $\phi_{pL}(\rho, t)$ are obtained to simulate NT and ΔT, thereby being compared with the experimental data.

Experimental results of NT and ΔT for C_{70}/toluene solution are shown in Fig. 3 as solid points. The NT data shown in Fig. 3(a) are obtained by integrating the intensity distribution over the exposed pixels of CCD. In Fig. 3(a), NT shows a steep drop near the zero delay time region and then follows a slow recovery as t_d increases. And the normalized enhanced transmission ΔT data at various values of delay time t_d are shown in Fig. 3(b). ΔT increases to about 0.03 at zero delay time because of the Kerr refraction of toluene. Then, it decreases abruptly to about –0.1. Subsequently, it gradually increases to a constant level.

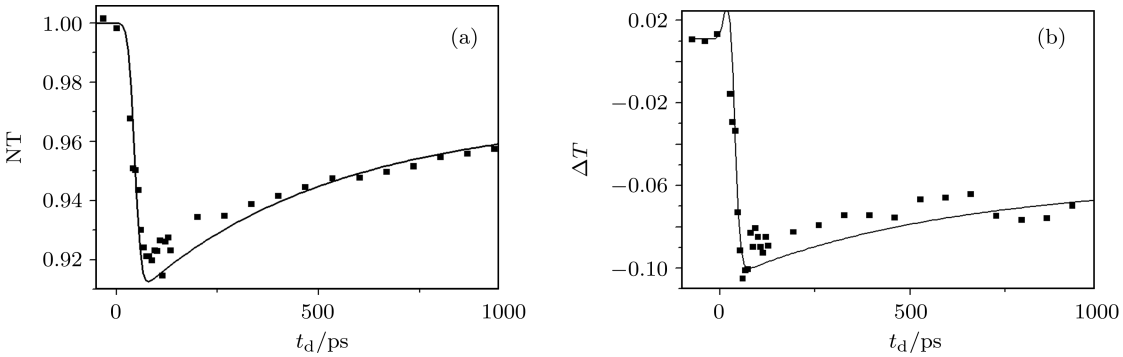


Fig. 3. (a) NT, the normalized transmittance, and (b) ΔT, transmittance contrast plotted versus delay time t_d for C_{70}/toluene solution, where dots denote experimental data, and curves represent theoretical fits.

The nonlinear absorptive and refractive dynamics in the C_{70}/toluene solution decide the dependence of NT and ΔT on t_d. The rate equations describing various transition processes are given as follows:

$$\frac{dN_{S_0}}{dt} = -\frac{\sigma_{S_0} I_e N_{S_0}}{\hbar\omega} - \frac{\beta I_e^2}{2\hbar\omega} + \frac{N_{S_1}}{\tau_{S_1}} + \frac{N_{T_1}}{\tau_{T_1}}, \quad (10)$$

$$\frac{dN_{S_1}}{dt} = -\frac{\sigma_{S_1} I_e N_{S_1}}{\hbar\omega} + \frac{\sigma_{S_0} I_e N_{S_0}}{\hbar\omega} - \frac{N_{S_1}}{\tau_{S_1}} - \frac{N_{S_1}}{\tau_{ISC}} + \frac{N_{S_n}}{\tau_{S_n}}, \quad (11)$$

$$\frac{dN_{S_n}}{dt} = \frac{\sigma_{S1} I_e N_{S_1}}{\hbar\omega} + \frac{\beta I_e^2}{2\hbar\omega} - \frac{N_{S_n}}{\tau_{S_n}}, \quad (12)$$

$$\frac{\mathrm{d}N_{\mathrm{T}_1}}{\mathrm{d}t} = -\frac{\sigma_{\mathrm{T}_1} I_{\mathrm{e}} N_{\mathrm{T}_1}}{\hbar\omega} - \frac{N_{\mathrm{T}_1}}{\tau_{\mathrm{T}_1}} + \frac{N_{\mathrm{S}_1}}{\tau_{\mathrm{ISC}}} + \frac{N_{\mathrm{T}_n}}{\tau_{\mathrm{T}_n}}, \quad (13)$$

$$\frac{\mathrm{d}N_{\mathrm{T}_n}}{\mathrm{d}t} = \frac{\sigma_{\mathrm{T}_1} I_{\mathrm{e}} N_{\mathrm{T}_1}}{\hbar\omega} - \frac{N_{\mathrm{T}_n}}{\tau_{\mathrm{T}_n}}, \quad (14)$$

where τ_i is the lifetime of state I, τ_{ISC} is the intersystem crossing time from singlet state S_1 to triplet state T_1, $\hbar$ is the Planck constant, ω is the laser frequency, and I_{e} denotes the pump intensity.

To fit the NT and ΔT experimental data, the populations, the absorption cross sections and the lifetimes of various energy levels, as well as the intersystem crossing time and the change of refractive index per unit density should be adjusted. The set of differential equations should be solved numerically. Since the intersystem crossing time is about one nanosecond, the population density of triplet state can be neglected in the picosecond time range. $\sigma_{\mathrm{S}_0} = 3.8\times10^{-21}$ cm^2 is set as mentioned in Ref. [9]. Firstly, NT and ΔT are calculated by varying the values of σ_{S_1}, σ_{T_1}, τ_{S_1}, β, $\Delta\eta_{\mathrm{S}_1}$ and $\Delta\eta_{\mathrm{T}_1}$, until the best fit to experimental data is obtained. Then the intensity and the phase of the probe beam can be obtained by using the fit value in Eqs. (7)–(9).

It is found that the best fit occurs when $\sigma_{\mathrm{S}_1} = 4.9\times10^{-17}$ cm^2, $\sigma_{\mathrm{T}_1} = 4.9\times10^{-17}$ cm^2, $\tau_{\mathrm{S}_1} = 0.7$ ns, $\beta = 0$, $\Delta\eta_{\mathrm{S}_1} = -2.3\times10^{-22}$ cm^3 and $\Delta\eta_{\mathrm{T}_1} = -3.9\times10^{-22}$ cm^3. $\beta = 0$ indicates that the nonlinear absorption originates from the excite-state dynamics. The result that σ_{S_1} is greater than σ_{S_0} indicates that the excited-state absorption of S_1 causes the steep drop observed in the NT experimental data. The subsequent slow recovery from the valley bottom of NT can be interpreted by the long lifetime of the triplet state T_1, which is on the order of 10^{-2} s.[18] The value of $\Delta\eta_{\mathrm{S}_1}$ implies why ΔT decreases abruptly near the zero delay time region. The subsequent increase to a constant level is because of the long lifetime and large $\Delta\eta_{\mathrm{T}_1}$ of T_1 state.

From the above explanation, it is found that the absorption and the refraction of excited-state determine the nonlinear process in picosecond time range. σ_{S_1} and $\Delta\eta_{\mathrm{S}_1}$ of the singlet excited state S_1 are critical factors to affect the nonlinear behaviour of C_{70} molecules near the zero delay time region. But populations of S_1 will rapidly relax back to S_0 or transfer to the lowest excited triplet state T_1 by intersystem crossing. Then, populations will accumulate in state T_1 because of its long lifetime. Thus, the long transmittance tail of NT and the long increase of ΔT, which occur in nanosecond time range, are determined by σ_{T_1} and $\Delta\eta_{\mathrm{T}_1}$.

The photophyscial parameters obtained by 4f-NIT-PO and listed in Table 1, are in agreement with the ones reported in the earlier literature. $\Delta\eta_{\mathrm{S}_1}$ and $\Delta\eta_{\mathrm{T}_1}$ are obtained only in the present system.

Table 1. Photophysical parameters obtained by fitting the pump-probe experimental data to the theoretical formula. The published values of C_{70}, cited from Ref. [7], are also listed there for comparison.

	this work	Ref. [7]
σ_{S_0}/cm^2	3.8×10^{-17}	3.5×10^{-17}
σ_{S_1}/cm^2	4.9×10^{-17}	$(6.0\pm0.5)\times10^{-17}$
σ_{T_1}/cm^2	4.9×10^{-17}	$(4.2\pm0.1)\times10^{-17}$
$\Delta\eta_{\mathrm{S}_1}$/cm^3	-2.3×10^{-22}	
$\Delta\eta_{\mathrm{T}_1}$/cm^3	-3.9×10^{-22}	
n_2/(cm^2/GW)	0.8×10^{-18}	
τ_{S_1}/ns	0.7	0.65
τ_{ISC}/ns	1.2	0.65

The population evolutions of C_{70} in various states during the determination of photophyscial parameters as shown in Fig. 4, are obtained for a better interpretation of the optical process in picosecond time range. When the pump pulse passes through the nonlinear sample, the absorption of S_0 excites the population from S_0 to S_1. This absorption causes the steep drop in the transmission intensity. Then, the population of S_1 relaxes back to S_0 or makes intersystem-crossing transition to the lowest excited triplet state T_1. The population will accumulate in state T_1 within picosecond time range.

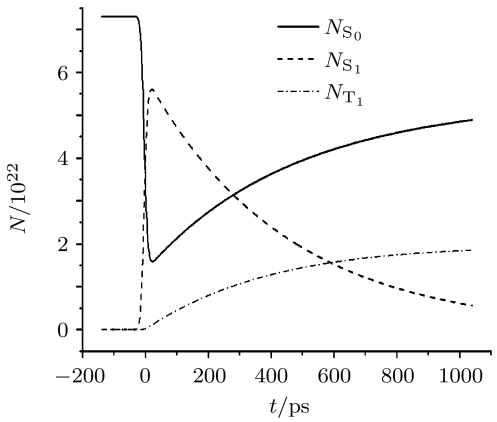


Fig. 4. Populations of states N_{S_0}, N_{S_1} and N_{T_1}, calculated from the rate equations and the photophysical parameters determined from the theoretical fit.

4. Summary

The picosecond time-resolved pump-probe system based on $4f$ nonlinear imaging technique with phase object is introduced to measure the optical nonlinearities of C_{70}/toluene solution. This modified system can be used to measure the dynamic nonlinear absorption and refraction of the excited-state simultaneously. A five-level model is adopted to interpret the experimental data of NT and ΔT. It is found that σ_{S_1} and $\Delta\eta_{S_1}$ of the singlet excited state S_1 determine the nonlinear absorption and refraction respectively while the delay time is on the picosecond time scale. Because of the short lifetime of the excited singlet state S_1 and a rapidly intersystem crossing, populations should accumulate in the excited triplet state T_1, which has a rather long lifetime. Then, the nonlinear behaviour of C_{70} is determined by σ_{T_1} and $\Delta\eta_{T_1}$ while the delay time comes to the nanosecond time scale. The values of $\Delta\eta_{S_1}$ and $\Delta\eta_{T_1}$, which denote the changes of refraction index per unit density of states S_1 and T_1, are obtained in the present system by numerical simulation. We find that the coefficients $\Delta\eta_{S_1}$ and $\Delta\eta_{T_1}$ play a very important role in the nonlinear refraction of C_{70}/toluene solution.

References

[1] Seshadri R, Rao C N R, Pal H, Mukherjee T and Mittal J P 1993 *Chem. Phys. Lett.* **205** 395

[2] Watanabe A, Ito O, Watanabe M, Saito H and Koishi M 1996 *J. Phys. Chem.* **100** 10518

[3] Tanigaki K, Ebbesen T W and Kuroshima S 1991 *Chem. Phys. Lett.* **185** 189

[4] Gevaert M and Kamat P V 1992 *J. Phys. Chem.* **96** 9883

[5] Lee M, Song O K, Seo J C, Kim D, Su Y D, Jin S M and Kim S K 1992 *Chem. Phys. Lett.* **196** 144

[6] Ganeev R A, Ryasnyansky A I, Kodirov M K and Usmanov T 2000 *Opt. Commun.* **185** 473

[7] Reindl S, Penzkofer A and Gratz H 1998 *Photochemistry and Photobiology* A: *Chemistry* **115** 89

[8] Bindhu C V, Harilal S S, Nampoort V P N and Vallabhan C P G 2000 *Appl. Phys.* B **70** 429

[9] Foley S, Santos M N B, Fedorov A, Bensasson R V, Leach S and Gigante B 2000 *Chem. Phys.* **263** 437

[10] Boudebs G and Cherukulappurath S 2004 *Phys. Rev.* A **69** 053813

[11] Yang J Y, Gu J H, Song Y L, Shi G, Wang Y X, Zhang W and Lang J P 2007 *J. Phys. Chem.* B **111**(28) 7987

[12] Li Y B, Pan G, Yang K, Zhang X, Wang Y X, Wei T H and Song Y L 2008 *Opt. Express* **16** 6251

[13] Shi G, Li Y B, Yang J Y, Wang Y X, Song Y L and Wang C H 2009 *J. Opt. Soc. Am.* B **26**-3 420

[14] Yang J Y, Song Y L and Gu J H 2009 *Chin. Phys.* B **18** 2828

[15] Yang J Y, Song Y L Jin X Shui M and Li C W 2010 *Chin. Phys.* B **19** 024201

[16] Sheik-Bahae M, Wang J, DeSalvo R, Hagan D J and Stryland E W V 1992 *Opt. Lett.* **17** 258

[17] Wang J, Sheik-Bahae M, Said A A, Hagan D J and Stryland E W V 1994 *J. Opt. Soc. Am.* B **11**(6) 1009

[18] Etheridge H T and Weisman R B 1995 *J. Phys. Chem.* **99** 2782